Published in final edited form as:
Mech Dev. 2010 ; 127(5-6): 292–300. doi:10.1016/j.mod.2010.03.001.

Tbx1 is Necessary for Palatal Elongation and Elevation

Steven Goudy[1], **Amy Law**[2], **Gabriela Sanchez**[1], **H. Scott Baldwin**[3,4], and **Christopher Brown**[3]

[1]Department of Otolaryngology, Vanderbilt University School of Medicine, Nashville, TN

[2]University of Louisville School of Medicine, Louisville, KY

[3]Department of Pediatrics, Division of Pediatric Cardiology, Vanderbilt University School of Medicine, Nashville, TN

[4]Department of Cell and Developmental Biology, Vanderbilt University School of Medicine, Nashville, TN

Abstract

The transcription factor TBX1 is a key mediator of developmental abnormalities associated with DiGeorge/Velocardiofacial Syndrome. Studies in mice have demonstrated that decreased dosage of *Tbx1* results in defects in pharyngeal arch, cardiovascular, and craniofacial development. The role of *Tbx1* in cardiac development has been intensely studied; however, its role in palatal development is poorly understood. By studying the *Tbx1*-/- mice we found defects during the critical points of palate elongation and elevation. The intrinsic palate defects in the *Tbx1*-/- mice were determined by measuring changes in palate shelf length, proliferation, apoptosis, expression of relevant growth factors, and in palate fusion assays. *Tbx1*-/- embryos exhibit cleft palate with failed palate elevation in 100% and abnormal palatal-oral fusions in 50%. In the *Tbx1*-/- mice the palate shelf length was reduced and tongue height was greater, demonstrating a physical impediment to palate elevation and apposition. In vitro palate fusion assays demonstrate that *Tbx1*-/- palate shelves are capable of fusion but a roller culture assay showed that the null palatal shelves were unable to elongate. Diminished hyaluronic acid production in the *Tbx1*-/- palate shelves may explain failed palate shelf elevation. In addition, cell proliferation and apoptosis were perturbed in *Tbx1*-/- palates. A sharp decrease of *Fgf8* expression was detected in the *Tbx1*-/- palate shelves, suggesting that *Fgf8* is dependent on *Tbx1* in the palate. *Fgf10* is also up-regulated in the *Tbx1*-/- palate shelves and tongue. These data demonstrate that *Tbx1* is a critical transcription factor that guides palatal elongation and elevation and that *Fgf8* expression in the palate is *Tbx1*-dependent.

Keywords

palate; *Tbx1*; *Fgf8*; *Tgfb3*; *Fgf10*; *Shh*; *Hyaluronic Acid*

Corresponding Author: steven.l.goudy@vanderbilt.edu, Steven Goudy, Department of Otolaryngology 7209 MCE South Tower 1215 21st Ave South Nashville, TN 37232 fax 615-343-9725.

Introduction

Cleft palate is one of the most commonly observed congenital malformations in humans, occurring in up to 1 in 500 live births(Schutte and Murray, 1999). The function of the palate is to separate the oral cavity and nasal cavity to allow respiration, deglutition and phonation to occur. Craniofacial development is a highly regulated process involving the growth and fusion of the maxillary, mandibular and nasal processes(Chai and Maxson, 2006). Specifically, the migration of the cranial neural crest mesenchyme through the facial primordium guides proper facial growth(Trainor, 2005). During facial morphogenesis, paired first brachial arches elongate and fuse in the midline to create the palate and mandible.

During palate development, paired palate shelves under go a carefully orchestrated expansion, elevation, and midline fusion between E13.5 and E15.5 in mice. This process involves proliferation of mesenchyme within the palate shelves, and dissolution of the epithelium during palate fusion(Nawshad, 2008). Interruption of the normal palate proliferation, elevation or fusion process leads to cleft palate formation. Many genes have been identified as critical to palate development, including the transcription factor *Tbx1*(Gritli-Linde, 2007).

The T-box transcription factor TBX1 has been linked to DiGeorge and Velocardiofacial Syndrome in humans, both of which have cardiac and cleft palate phenotypes, similar to the mouse phenotype (Jerome and Papaioannou, 2001; Merscher *et al.*, 2001). The cardiac anomalies in *Tbx1*-/- mice occur, in part, due to changes in *Fgf8* and *Fgf10* expression, suggesting that *Fgf8* and *Fgf10* are involved in *Tbx1* signaling (Aggarwal *et al.*, 2006; Brown *et al.*, 2004). *Tbx1* expression is observed throughout the developing face, including the epithelium and mesenchyme of the maxillary and mandibular prominences, as well as the endoderm of the pharyngeal pouches (Chapman et al., 1996). In the palate, *Tbx1* is strongly expressed in the palatal epithelium and mesenchyme, but the underlying role(s) of *Tbx1* in palate development is unknown (Zoupa et al., 2006). *Tbx1* has cell-autonomous effects in the pharyngeal endoderm where it is expressed. Specific deletion of *Tbx1* from the pharyngeal endoderm leads to fourth pharyngeal arch anomalies, cleft palate and abnormal facial musculature development (Arnold *et al.*, 2006; Zhang *et al.*, 2005). However, *Tbx1* has a non-cell autonomous role in guiding neural crest migration during cardiac morphogenesis (Vitelli et al., 2002). Thus, despite previous investigations, the etiology of the cleft palate in *Tbx1*-/- mice is still unclear.

We have hypothesized that *Tbx1* is necessary for normal palatal elongation and elevation. In this study, we demonstrate that cleft palate in *Tbx1*-/- mice is associated with failed palatal elevation, likely due to decreased palatal width, increased tongue height, and palatal-oral fusions. This may be due, in part, to diminished hyaluronic acid production, decreased palatal *Fgf8* expression, increased *Fgf10* expression, and altered proliferation/apoptosis. These results suggest that *Tbx1* is a key transcription factor necessary for normal palate development.

Results

Tbx1-/- mice display a primary defect in palate elongation and elevation

To better understand the role of *Tbx1* in palate development, we examined the palate phenotype in *Tbx1*-/- mice. The *Tbx1* null embryos all exhibit a cleft palate (N=20/20). Palatal shelves are formed in *Tbx1*-/- embryos, but the shelves appear shortened, and are unable to elongate and elevate (figure 1 C, D). Additionally, the palatal shelves of null embryos were found to have posterior fusions to the oral cavity in 50% (N=10/20 embryos) (figure 1 D). The etiology of the palatal defect from E13.5-E15.5 was failure of elevation of the palate shelves (N=20/20).

In figure 2 the width of the palate shelves and the height of the tongue musculature were measured to determine if shortened palate shelves or tongue obstruction were potential mechanisms of cleft palate formation. In the E14.5 wild type mice we observed normal palate shelf elevation and tongue down-growth (figure 2 A, B, C). In the *Tbx1*-/- mice we observed failed palate shelf elevation, shortened palate shelves and increased tongue musculature height (figure 2 D, E, F). Measurements from the anterior, middle and posterior palate shelves and tongue musculature demonstrated significant differences in the *Tbx1*-/- mice. The palate shelves of the *Tbx1*-/- mice were significantly shorter in the middle and posterior palate (figure 2 G). The height of the tongue musculature in the *Tbx1*-/- mice was significantly greater in the anterior and middle tongue (figure 2 H). We measured E13.5 palate shelf length and tongue height and did not detect a statistical difference (data not shown).

In vitro palate fusion assays were carried out to determine if proper palate fusion could occur in the *Tbx1*-/- mice. Using a filter culture technique in which the palatal shelves are isolated and artificially apposed, we found that the *Tbx1*-/- palatal shelves were capable of undergoing fusion when compared to controls (N=4/4) (figure 3 A, B). Using the roller bottle technique allowed us to study the palatal shelves in situ, with the tongue removed, identifying whether the palate shelves can properly elongate and fuse. In the roller bottle palate cultures we found that *Tbx1*-/- palatal shelves were unable to elongate and fuse compared to controls (N=4/4) (figure 3 C, D).

To determine if poor hydrostatic turgor of *Tbx1*-/- palate shelves contributed to poor palate shelf elongation and failed elevation we used alcian blue staining in the *Tbx1*-/- mice to detect hyaluronic acid. Coronal sections of E13.5 wild-type mice demonstrated abundant hyaluronic acid staining in the anterior and posterior palate shelves (figure 4 A, C). However, there was diminished intensity of hyaluronic acid staining in the E13.5 anterior and posterior palate shelves of the *Tbx1*-/- mice (figure 4 B, D). The E13.5 wild-type and *Tbx1*-/- coronal sections were also treated with hyaluronidase, demonstrating no alcian blue staining in the palate, confirming that the blue staining represents hyaluronic acid (data not shown).

Abnormal palatal elongation and elevation is associated with alterations in proliferation and apoptosis

To assess if cell proliferation was altered in *Tbx1*-/- embryos, we examined proliferation rates using phosphohistone-H3 immunohistochemistry. Cell proliferation was elevated at E12.5 and E13.5 in *Tbx1*-/- palatal shelves (p=0.001) (figure 5 A, C, D). To determine if alterations in programmed cell death were associated with the *Tbx1*-/- phenotype, we assessed apoptosis using TUNEL staining on *Tbx1*-/- palatal shelves (figure 5 B, E). Palatal shelf apoptosis was normal at E12.5 but elevated in E13.5 *Tbx1*-/- embryos (p=0.02) (figure 5 F).

Tbx1-/- palates display discrete abnormalities in *Fgf8* and *Fgf10*

To determine targets of *Tbx1* signaling we investigated changes in candidate growth factors necessary during palate development (figure 6). Using *in situ* hybridization, we evaluated the expression patterns of *Fgf10, Fgf8, Shh,* and *Tgfb3* in *Tbx1*-/- mice. *Fgf8* expression was greatly decreased in the absence of *Tbx1* (figure 6 A, B). *Fgf10* expression was increased in the midline of the tongue and the nasal aspect of the palate shelves of *Tbx1*-/- mice (figure 6 C, D). *Shh* expression was unchanged in the *Tbx1*-/- palate shelves (figure G, H). *Tgfb3* is diminished in the mandible and skull base (figure 6H astericks) but still present in the medial edge epithelium (MEE) (figure 6F arrows).

Discussion

Without *Tbx1*, normal palate development fails to occur. In this paper we show that *Tbx1* is necessary for palatal elongation and elevation. To support this, we identified phenotypic changes in palate shape, and behavior. In addition we identified intrinsic differences in palate composition and growth factor expression that explain, in part, the *Tbx1*-/- palate phenotype.

Tbx1 Palate Shelves are Incapable of Elongation and Elevation

Palatal development is dependent on coordination of palatal elongation, elevation, and fusion. Morphologically we demonstrate shortened palatal shelves that fail to elongate and elevate characterize the *Tbx1*-/- cleft palate phenotype (figure 1). Furthermore palatal-oral fusions occur in 50% of mice, tethering the posterior palate (figure 1D, 2F). The presence of palatal-oral fusions suggests that *Tbx1* acts to maintain epithelial integrity in the posterior palate. Palatal-oral adhesions leading to cleft palate formation have been demonstrated in *Fgf10*, *Jagged2* and *Irf6* knock-out mice, all of which have defective epithelial development but, unlike the *Tbx1*-/- mice, maintain epithelial integrity (Ingraham et al., 2006;Jiang et al., 1998;Rice et al., 2004;Richardson et al., 2009;Richardson et al., 2006). *Irf6* and *Jagged2* were found to work together to maintain peridermal cell viability, preventing palatal-oral adhesions. However, areas of fusion between the palate shelves and the tongue and oral cavity have been found in the *Irf6*-/- and *Fgf10*-/- mice (Alappat et al., 2005;Richardson et al., 2009). The palatal-oral fusions in *Tbx1*-/- animals may directly prevent normal palatal elevation, therefore contributing to cleft palate formation. However, all of the *Tbx1*-/- mice have a cleft palate but the presence of the palatal-oral fusions was detected in only 50% of *Tbx1*-/- mice and that palate fusion typically occurs from anterior to posterior, suggests that palatal-oral fusions alone do not lead to cleft palate formation in the *Tbx1*-/- mice.

In the *Tbx1*-/- mice there are quantifiable differences in the palate width and tongue height. Palate shelf width in the E14.5 *Tbx1*-/- mice was significantly shorter in the middle and posterior regions (figure 2 G). Tongue musculature height in the *Tbx1*-/- mice was significantly greater in the anterior and middle regions (figure 2 H). The lack of palatal lengthening and palatal-oral fusions discussed above suggests two separate mechanisms that might contribute to inhibition of palate elevation in the *Tbx1* -/- mice. In addition, lack of tongue down-growth in the *Tbx1* -/- mice results in lingual interference with proper palate elevation providing a third mechanism contributing to the cleft palate phenotype. This data suggests that not only is palate development affected by *Tbx1* deletion, but that tongue development is aberrant as well. The failure of tongue down growth causing cleft palate formation has been demonstrated in other mouse models (Huang et al., 2008). In *Tbx2* deficient mice cleft palate also occurs due to deficient palatal shelves. At e14.0 the *Tbx2*-/- palate shelves were statistically smaller, leading to cleft palate(Zirzow et al., 2009). The *Tbx2*-/- palate phenotype is similar to the *Tbx1*-/- phenotype shown in figure 2, however the tongue shape was not assessed in the *Tbx2*-/- mutants.

Palate Culture Assays Demonstrate Shortened Palate Shelves in *Tbx1*-/- mice

Use of two palate culture techniques demonstrated that *Tbx1*-/- palate shelves are capable of fusion, and the primary pathology is failed palatal elongation. There were marked differences in palate culture assay when we compared filter and roller bottle assays (figure 3). The filter culture assay showed that the *Tbx1*-/- palate shelves are capable of undergoing fusion, despite there being delayed apoptosis in the *Tbx1*-/- palate shelves (figure 5). However, the roller culture assay demonstrated that the *Tbx1*-/- palate shelves fail to elongate and fuse, even when palatal-oral fusions were not a restriction. These data suggest that the primary pathology present in the *Tbx1*-/- mice palates is due to failed palatal elongation and elevation. This is similar to the *Tbx2*-/- mice, the palatal shelves were able to fuse in apposition, however the roller bottle technique was not used to identify primary palatal insufficiency(Zirzow et al., 2009).

Diminished Hyaluronic Acid in *Tbx1-/-* Palate Shelf May Impair Elevation

Elevation of the palate shelves is proposed to occur due to the proliferative and hydrostatic forces within the palate. Hydration of extracellular matrix components, including hyaluronan and chondroitin sulfate proteoglycans, has been suggested to provide an elevating turgor pressure within the palatal shelves (Morris-Wiman and Brinkley, 1992). In figure 4 we show that the E13.5 *Tbx1*-/- palatal shelves have diminished hyaluronic acid (**B, D**) compared to the wild-type palate shelves (**A, C**). Decreased hyaluronic acid content of the *Tbx1*-/- palate shelves likely contributes to their decreased width and failed elevation. This provides a potential mechanism contributing to cleft palate formation in the *Tbx1*-/- mice and is, to our knowledge, the first demonstration of altered extracellular matrix in the *Tbx1* mutant palate.

Abnormal Proliferation and Apoptosis in the *Tbx1-/-* Palate shelves

To identify the underlying defect in palate development we examined if alterations in proliferation or apoptosis may be an etiologic factor leading to cleft palate formation. In figure 5 we demonstrate an increase in proliferation at E12.5 and E13.5 in the *Tbx1*-/- palate shelves. In the palate, proliferation is mostly confined to the neural crest derived mesenchyme, suggesting that the absence of *Tbx1* in the palate induces the neural crest to proliferate (Dudas *et al*., 2007;Ito *et al.*, 2003). This data is contrary to the observed decrease in cell proliferation during cardiac development in *Tbx1* nulls, suggesting that *Tbx1* may act on the cranial neural crest in a context dependent manner that is different than its role during palatogenesis (Vitelli et al., 2002). In *Fgf10*-/- mice, there was decreased palatal proliferation at E12.5 and E13.5, suggesting that *Fgf10* may induce cellular proliferation in the palate (Rice et al., 2004). Increased *Fgf10* expression (discussed below) in the *Tbx1*-/- palate shelves may explain the increased cellular proliferation observed in figure 5. In the *Tbx2*-/- palate shelves there is also increased cellular proliferation at E12.5, suggesting that cellular proliferation alone does not account for alterations in palatal size (Zirzow et al., 2009).

In the *Tbx1*-/- palatal shelves, there is a significant increase in apoptosis in day E13.5. The premature increase in apoptosis at E13.5 may allow for epithelial break down in the lateral palate shelves and oral cavity leading to aberrant fusion demonstrated in figures 1D and 2F. In the *Tbx2*-/- mutants increased apoptosis was identified at e11.5 and e12.5, demonstrating a similar pattern of cellular changes seen in the *Tbx1*-/- mutant mice (Zirzow et al., 2009).

Altered *Fgf8* and *Fgf10* Expression in *Tbx1-/-* Palate Shelves

To identify the targets of *Tbx1* function in the palate shelves we evaluated the *Tbx1*-/- palate shelves for altered expression of *Shh, Tgfb3, Fgf8*, and *Fgf10*. In the *Tbx1*-/- mice we observed increased palatal and tongue mesenchymal *Fgf10* expression (figure 6 C, D) but marked down-regulation of *Fgf8* in the palate epithelium (figure 6 A, B). *Tbx1* acts upstream of *Fgf10* and *Fgf8* in heart development, and others have shown that *Fgf8* and *Fgf10* are required for normal palatal development (Alappat *et al.*, 2005; Brown *et al.*, 2004; Rice *et al.*, 2004). Conditional deletion of *Tbx1* from the pharyngeal epithelium led to a loss of *Fgf8* expression and was concomitant with aberrant pharyngeal pouch development and outgrowth (Arnold et al., 2006). Investigation of *Tbx1*+/-; *Fgf10*+/-; *Fgf8*+/- mice showed a possible functional redundancy between *Fgf10* and *Fgf8* during pharyngeal arch development. Loss of *Fgf8* expression in pharyngeal arch development leads to increases in apoptosis, suggesting that *Tbx1* may provide a cell-protective effect in the palate epithelium (Abu-Issa et al., 2002). Diminished *Fgf8* expression in the palatal epithelium of *Tbx1*-/- mice may explain the increase in apoptosis we observed (figure 5), similar to the findings in pharyngeal arch development. Notably, loss of *Fgf8* signaling in the MEE in the *Tbx1*-/- mice occurs in the same region as the palatal-oral fusions. Expression of *Tgfb3* in the *Tbx1*-/- mice is still present in the MEE but reduced in the mandibular, and skull base mesenchyme. Loss of *Fgf10* expression has been shown to alter the location of *Tgfb3* signaling in the posterior palate MEE but the increased

Fgf10 expression seen in the *Tbx1-/-* palatal shelves has not altered *Tgfb3* palatal expression (Alappat et al., 2005).

Conclusion

Our data demonstrates that *Tbx1* is a key transcriptional mediator of palatal development. The finding of palatal-oral fusions, increased tongue height, decreased palatal width and impaired palatal elevation all cause physical impediments to normal palatal elevation and apposition, leading to cleft palate formation. The lack of normal hyaluronic acid in the *Tbx1*-/- palate shelves likely alters the normal palate length and turgor pressure necessary for palatal elevation and elongation. Absence of *Tbx1* leads to aberrant palatal proliferation and apoptosis that may be explained by decreased *Fgf8* expression and increased *Fgf10* expression. The palatal development and fusion assay clearly shows that the *Tbx1*-/- palatal shelves fail to elongate and elevate but are capable of fusion. These data taken together provide important insight into the role of *Tbx1* in palatogenesis and suggest several key processes that will require further elucidation.

Materials and Methods

Mice were maintained in a mixed background, and a 0600 to 1800 light-dark cycle was used. Noon of the day of observation of a vaginal plug was defined as E0.5. The *Tbx1* null mice were courtesy of Dr. Bernice Morrow. All procedures and animal experiments were approved by the Vanderbilt University Institutional Animal Care and Use Committee.

Palate and Tongue measurements

The E13.5 and E14.5 mice heads were fixed, embedded in paraffin, and were sectioned in a coronal plane (N=3 of wild type and *Tbx1* knockout). They were then hematoxylin and eosin stained. Digital photographs of the sections were taken using a Nikon e800 microscope with a Olympus digital capture system. The photographs were taken at 4× with a digital caliper placed on image with the Olympus software. Standardization of the anterior, middle and posterior palate images were performed. Using Adobe Photoshop CS3 the palate shelf width was measured using the lasso tool to outline the area of interest. Prior to measuring, we standardized the length using the Olympus digital caliper. The width of the palate and height of the tongue musculature were measured as demonstrated in figure 2 B and D. Specifically, the lateral extent of the palate shelf was determined by drawing a perpendicular line from the “hinge” region to the opposite palatal surface. The medial aspect of the palate shelf was defined as the level of the medial edge epithelium or the fusion plane of the palate. To account for palate orientation, all measurements were performed with the palate in a horizontal position, by rotating the un-elevated *Tbx1*-/- palate shelf images to a horizontal plane. The height of the tongue was measured from the digastric muscles inferiorly to the most superior aspect of the mid-tongue epithelium in the midline. Statistical analysis of the measurements was performed using Excel and a paired student t-test. Statistical significance was determined if $p<0.05$.

In Situ Hybridization—Evaluation of *Fgf10, Fgf8, and Shh* expression in both wild-type mice and *Tbx1*-/- mice was evaluated using in situ hybridization. After anesthetizing females using halothane, females were sacrificed using cervical dislocation. All complete embryos were fixed in 4% paraformaldehde (PFA) overnight and embedded in paraffin in preparation for *in situ* hybridization. Coronal sections were then prepared for *in situ* hybridization by rehydrating to PBS. Sections were treated with Proteinase K and refixed. After equilibration in tri-ethanolamine solution, sections are incubated in acetic anhydride to prevent nonspecific binding of the probe. Radioactive probe, both sense and antisense, was created using S35-dUTP. Sections were incubated overnight, followed by washings to remove unbound probe.

Slides were then developed on Kodak Biomax film to check for signal. If signal was present, sections were exposed to emulsion and incubated for 10-20 days depending on the strength of the radiographic signal before developing. The radioactive signal was evaluated using darkfield microscopy. Each section was photographed using a Nikon e800 microscope with an Olympus camera. The brightfield and darkfield images were merged using Olympus software.

Palate Culture

For the filter culture of the palatal shelves, E13.5 *Tbx1*-/- and wild type embryos were dissected in cold PBS. The palatal shelves were removed and placed in 0.4 μM filter culture wells (Falcon, Franklin Lakes, NJ). The palatal cultures were incubated in 1 ml of serum-free BGJb media (Gibco, Grand Island, NY) at the air-media interface. The cultures were incubated at 37 degrees with 95% O_2 5% CO_2 for 72 hours with the media changed every 24 hours. The cultures were then fixed with 4% paraformaldehyde for 2 hours at 4 degrees. The palates were serially dehydrated using ethanol, embedded in paraffin and then sectioned and stained with hematoxylin and eosin.

For roller culture of the palatal shelves, E13.5 *Tbx1*-/- and +/+ embryos were dissected in cold PBS. The mandibles and brain tissue were dissected free from the midface of each embryo. The remaining midface was placed in a roller bottle with 3 ml of serum-free BGJb. The cultures were incubated for 72 hours at 37 degrees with 95% O_2 and 5% C O_2 with media changes every 24 hours. The palatal cultures were fixed, sectioned, and stained as above.

Apoptosis and Proliferation Assays

To assess apoptosis, E12.5 and E13.5 *Tbx1*-/- (N=3) and +/+ (N=3) embryos were fixed and sectioned as mentioned above. Each section was TUNEL stained according to Roche protocol (Mannheim, Germany). Each embryo was sectioned from the primary palate to the end of the secondary palate. Each palate shelf was analyzed separately at 40×, and the plane of the lateral nasal wall and hinge region were used to determine the lateral edge of the palate shelf to be counted (area counted indicated by dotted line in figure 5 A, B, D, E).

To assess proliferation, E12.5 and E13.5 *Tbx1*-/- (N=3) and +/+ (N=3) embryos were fixed and sectioned as mentioned above. Each section was stained for phosphohistone H3 using the Cell Signaling protocol (Danvers, MA). The sections were then reviewed under 40× magnification and the number of proliferative cells per palate were counted in and identical fashion as above. Cell counts for *Tbx1*-/- and wild-type littermates were compared and assessed for statistical significance by Student's T-test.

Alcian Blue Staining

To assess the content of hyaluronic acid in the palate shelves, E13.5 wild-type and *Tbx1*-/- were fixed in 4% paraformaldehyde, embedded in paraffin and coronally sectioned. The sections were then dewaxed and were stained for alcian blue at pH 2.5 using the Dako Artisian staining protocol (Carpinteria, CA). Hyaluronidase (Sigma-Aldrich, St. Louis, MO) was used (50mg in 100ml PBS) was used to treat the slides for 1 hour at 37 C followed by the Dako protocol to remove hyaluronan.

Acknowledgments

The authors would like to thank Brian Schutte, Chin Chiang, Joey Barnett and Lance Prince for critically reading this manuscript. Expert technical assistance was performed by Kathleen Boyer and Yan Zhao. This work was supported by 1K08DE017953 and a Triological Career Development award to SG.

References

Abu-Issa R, Smyth G, Smoak I, Yamamura K, Meyers EN. Fgf8 is required for pharyngeal arch and cardiovascular development in the mouse. Development 2002;129:4613–25. [PubMed: 12223417]

Aggarwal VS, Liao J, Bondarev A, Schimmang T, Lewandoski M, Locker J, Shanske A, Campione M, Morrow BE. Dissection of Tbx1 and Fgf interactions in mouse models of 22q11DS suggests functional redundancy. Hum Mol Genet 2006;15:3219–28. [PubMed: 17000704]

Alappat SR, Zhang Z, Suzuki K, Zhang X, Liu H, Jiang R, Yamada G, Chen Y. The cellular and molecular etiology of the cleft secondary palate in Fgf10 mutant mice. Dev Biol 2005;277:102–13. [PubMed: 15572143]

Arnold JS, Werling U, Braunstein EM, Liao J, Nowotschin S, Edelmann W, Hebert JM, Morrow BE. Inactivation of Tbx1 in the pharyngeal endoderm results in 22q11DS malformations. Development 2006;133:977–87. [PubMed: 16452092]

Brown CB, Wenning JM, Lu MM, Epstein DJ, Meyers EN, Epstein JA. Cre-mediated excision of Fgf8 in the Tbx1 expression domain reveals a critical role for Fgf8 in cardiovascular development in the mouse. Dev Biol 2004;267:190–202. [PubMed: 14975726]

Chai Y, Maxson RE Jr. Recent advances in craniofacial morphogenesis. Dev Dyn 2006;235:2353–75. [PubMed: 16680722]

Chapman DL, Garvey N, Hancock S, Alexiou M, Agulnik SI, Gibson-Brown JJ, Cebra-Thomas J, Bollag RJ, Silver LM, Papaioannou VE. Expression of the T-box family genes, Tbx1-Tbx5, during early mouse development. Dev Dyn 1996;206:379–90. [PubMed: 8853987]

Dudas M, Li WY, Kim J, Yang A, Kaartinen V. Palatal fusion - where do the midline cells go? A review on cleft palate, a major human birth defect. Acta Histochem 2007;109:1–14. [PubMed: 16962647]

Gritli-Linde A. Molecular control of secondary palate development. Dev Biol 2007;301:309–26. [PubMed: 16942766]

Huang X, Goudy SL, Ketova T, Litingtung Y, Chiang C. Gli3-deficient mice exhibit cleft palate associated with abnormal tongue development. Dev Dyn 2008;237:3079–87. [PubMed: 18816854]

Ingraham CR, Kinoshita A, Kondo S, Yang B, Sajan S, Trout KJ, Malik MI, Dunnwald M, Goudy SL, Lovett M, Murray JC, Schutte BC. Abnormal skin, limb and craniofacial morphogenesis in mice deficient for interferon regulatory factor 6 (Irf6). Nat Genet. 2006

Ito Y, Yeo JY, Chytil A, Han J, Bringas P Jr, Nakajima A, Shuler CF, Moses HL, Chai Y. Conditional inactivation of Tgfbr2 in cranial neural crest causes cleft palate and calvaria defects. Development 2003;130:5269–80. [PubMed: 12975342]

Jerome LA, Papaioannou VE. DiGeorge syndrome phenotype in mice mutant for the T-box gene, Tbx1. Nat Genet 2001;27:286–91. [PubMed: 11242110]

Jiang R, Lan Y, Chapman HD, Shawber C, Norton CR, Serreze DV, Weinmaster G, Gridley T. Defects in limb, craniofacial, and thymic development in Jagged2 mutant mice. Genes Dev 1998;12:1046–57. [PubMed: 9531541]

Merscher S, Funke B, Epstein JA, Heyer J, Puech A, Lu MM, Xavier RJ, Demay MB, Russell RG, Factor S, Tokooya K, Jore BS, Lopez M, Pandita RK, Lia M, Carrion D, Xu H, Schorle H, Kobler JB, Scambler P, Wynshaw-Boris A, Skoultchi AI, Morrow BE, Kucherlapati R. TBX1 is responsible for cardiovascular defects in velo-cardiofacial/DiGeorge syndrome. Cell 2001;104:619–29. [PubMed: 11239417]

Morris-Wiman J, Brinkley L. An extracellular matrix infrastructure provides support for murine secondary palatal shelf remodelling. Anat Rec 1992;234:575–86. [PubMed: 1280922]

Nawshad A. Palatal seam disintegration: To die or not to die? that is no longer the question. Dev Dyn. 2008

Rice R, Spencer-Dene B, Connor EC, Gritli-Linde A, McMahon AP, Dickson C, Thesleff I, Rice DP. Disruption of Fgf10/Fgfr2b-coordinated epithelial-mesenchymal interactions causes cleft palate. J Clin Invest 2004;113:1692–700. [PubMed: 15199404]

Richardson RJ, Dixon J, Jiang R, Dixon MJ. Integration of IRF6 and Jagged2 signalling is essential for controlling palatal adhesion and fusion competence. Hum Mol Genet. 2009

Richardson RJ, Dixon J, Malhotra S, Hardman MJ, Knowles L, Boot-Handford RP, Shore P, Whitmarsh A, Dixon MJ. Irf6 is a key determinant of the keratinocyte proliferation-differentiation switch. Nat Genet 2006;38:1329–34. [PubMed: 17041603]

Schutte BC, Murray JC. The many faces and factors of orofacial clefts. Hum Mol Genet 1999;8:1853–9. [PubMed: 10469837]

Trainor PA. Specification and patterning of neural crest cells during craniofacial development. Brain Behav Evol 2005;66:266–80. [PubMed: 16254415]

Vitelli F, Morishima M, Taddei I, Lindsay EA, Baldini A. Tbx1 mutation causes multiple cardiovascular defects and disrupts neural crest and cranial nerve migratory pathways. Hum Mol Genet 2002;11:915–22. [PubMed: 11971873]

Zhang Z, Cerrato F, Xu H, Vitelli F, Morishima M, Vincentz J, Furuta Y, Ma L, Martin JF, Baldini A, Lindsay E. Tbx1 expression in pharyngeal epithelia is necessary for pharyngeal arch artery development. Development 2005;132:5307–15. [PubMed: 16284121]

Zirzow S, Ludtke TH, Brons JF, Petry M, Christoffels VM, Kispert A. Expression and requirement of T-box transcription factors Tbx2 and Tbx3 during secondary palate development in the mouse. Dev Biol. 2009

Zoupa M, Seppala M, Mitsiadis T, Cobourne MT. Tbx1 is expressed at multiple sites of epithelial-mesenchymal interaction during early development of the facial complex. Int J Dev Biol 2006;50:504–10. [PubMed: 16586352]

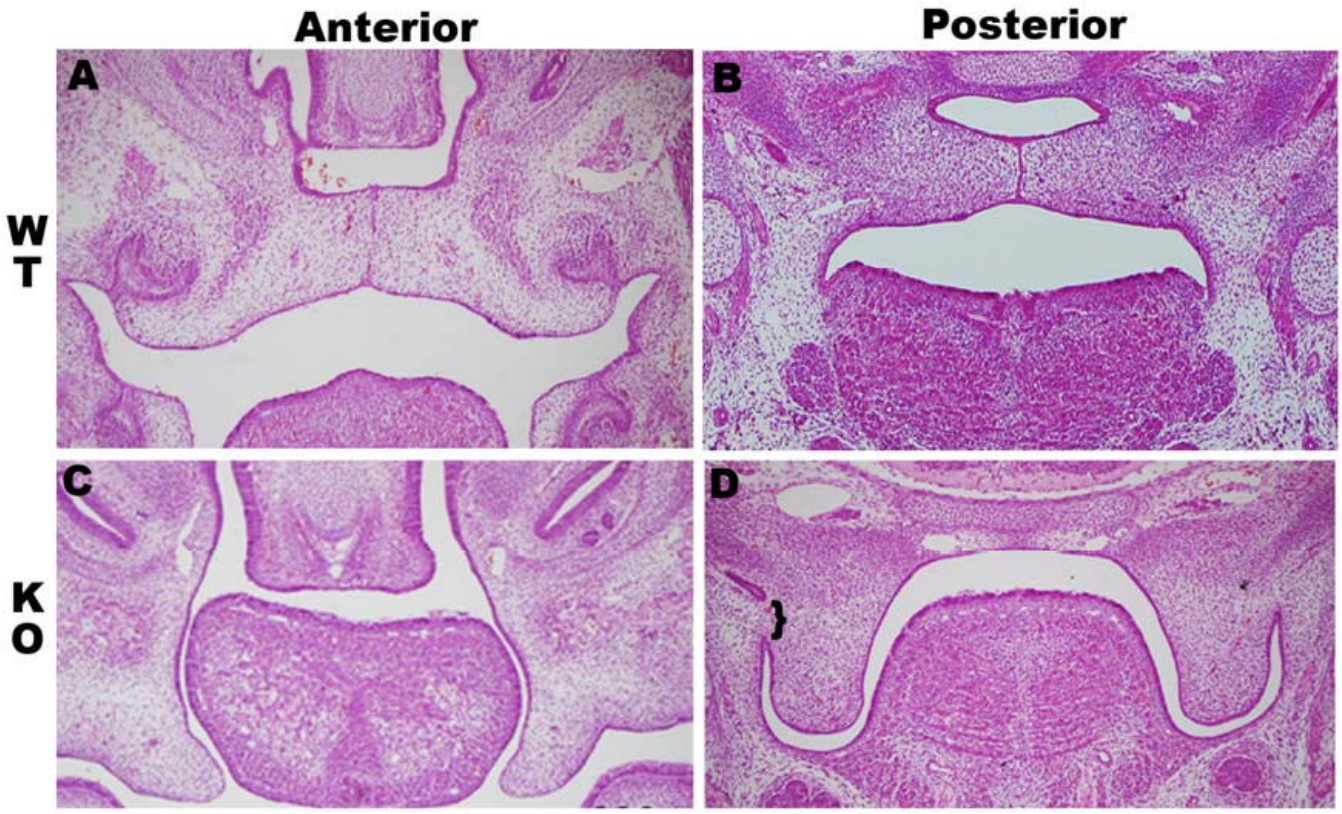

Figure 1. *Tbx1*-/- mice have cleft palates and palatal-oral fusion

(A+B) Coronal H & E section through E14.5 wild type palate shelves undergoing fusion anteriorly (A) and posteriorly (B). (C) Coronal sections through anterior palate of *Tbx1* -/- demonstrating the lack of palatal shelf elevation. (D) Posterior palate sections in *Tbx1* -/- mice showing palatal-oral fusion (bracket).

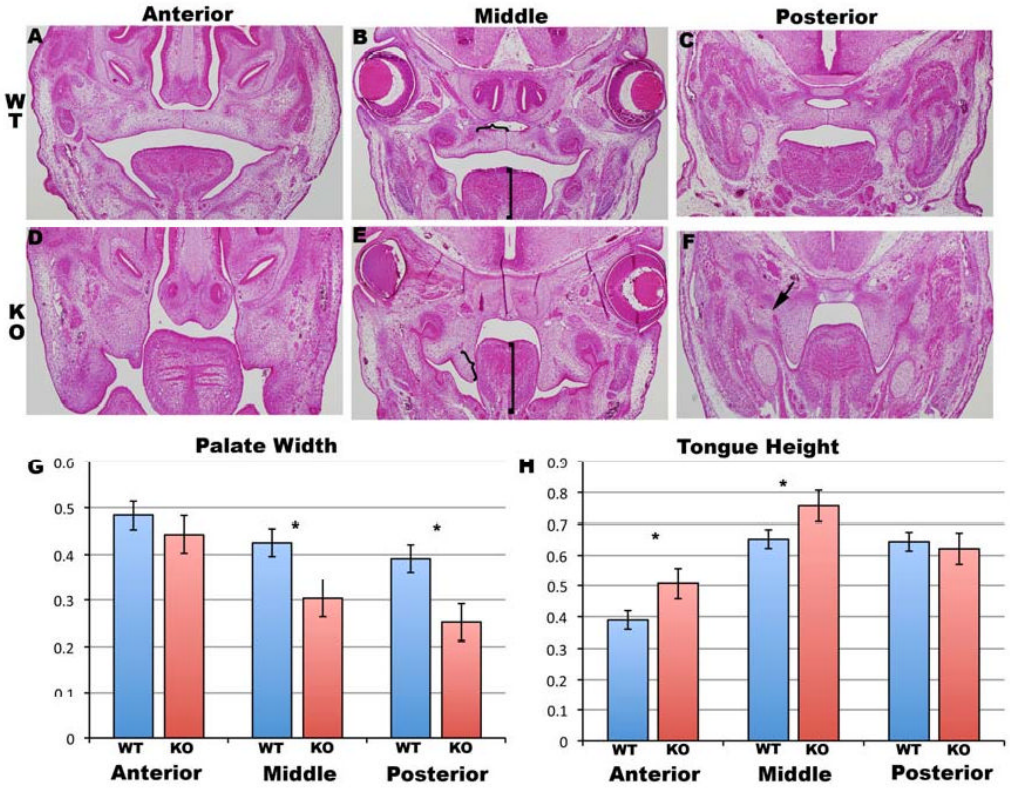

Figure 2. *Tbx1* -/- mice have shortened palates and greater tongue height

(A+B+C) Coronal H & E sections through E14.5 wild type palate shelves in the anterior (A), middle(B) and posterior(C) palate region. (D, E, F) Coronal sections through location matched (anterior, middle, posterior) palate regions in the *Tbx1*-/- mice. Measurements of palate width and tongue height were compared as demonstrated by the brackets on the palate (}) and tongue (]) in B and E. Statistical significance was denoted with * over the bar graphs in G and H. Note the posterior palatal-oral fusion in the in F (black arrow).

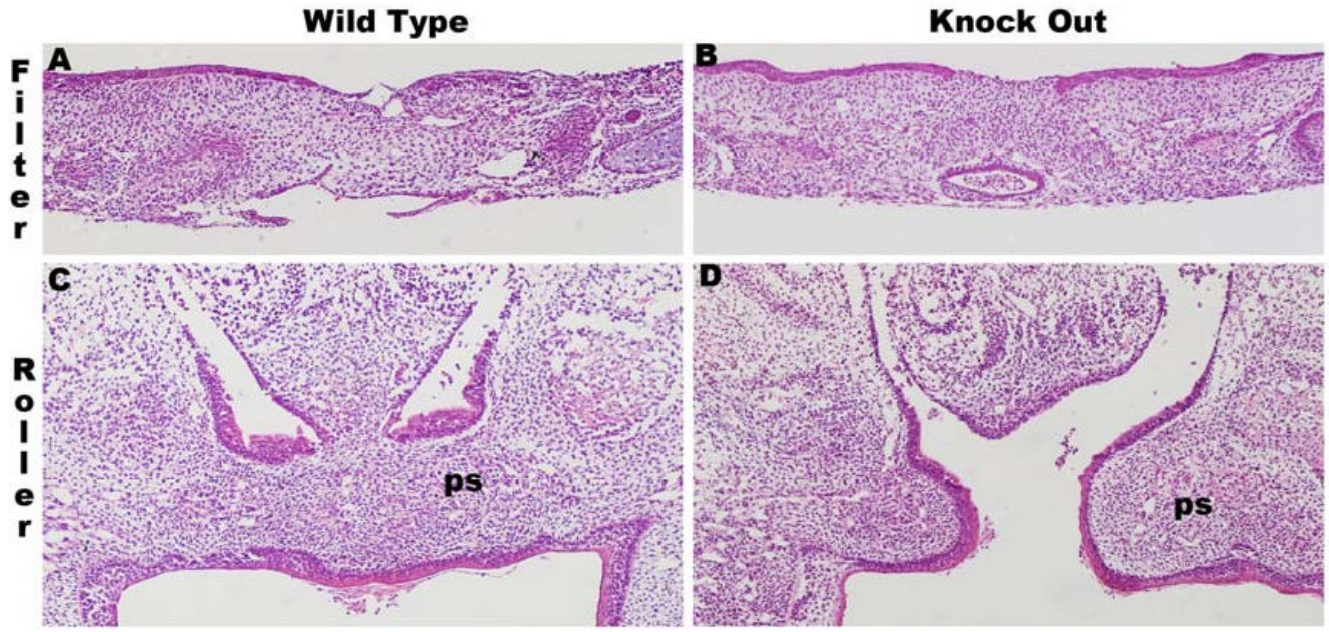

Figure 3. *Tbx1*-/- palatal shelves fail to develop in culture but are capable of fusion

Coronal sections with H&E staining of wild type palate (A) filter culture after 48-hour incubation. Note full fusion and confluence of mesenchyme. Filter cultured *Tbx1*-/-(B) palate shelves also demonstrating fusion. Wild type roller culture palate shelves demonstrating fusion (C) but *Tbx1*-/-(D) roller culture palate shelves that fail to fuse due to the inability of the palate shelves to appose. PS=palate shelf

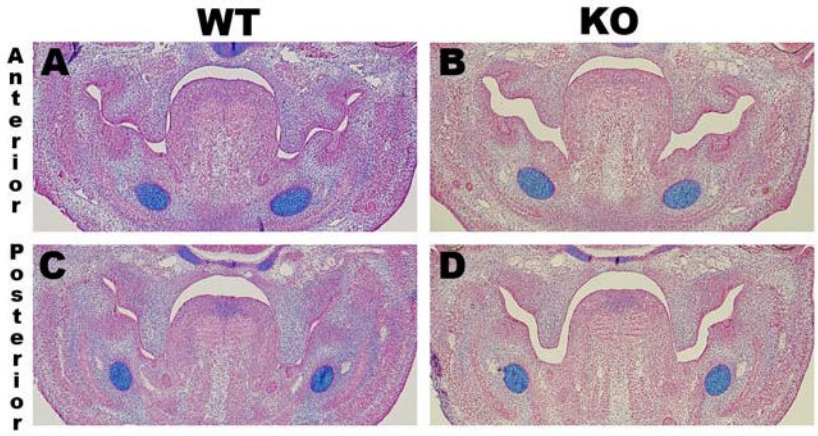

Figure 4. *Tbx1-/-* palate shelves have diminished hyaluronic acid staining

Coronal sections of E13.5 wild-type(A) anterior palate shelves showing diffuse alcian blue staining (arrow) as well as diffuse staining in the posterior palate shelves (C). In contrast, there is diminished alcian blue staining in the E13.5 *Tbx1-/-* palate shelves in the anterior (B) and posterior (D) regions. Treatment with hyaluronidase removed all alcian blue staining from the palate, indicating that the blue staining represents hyaluronic acid (data not shown).

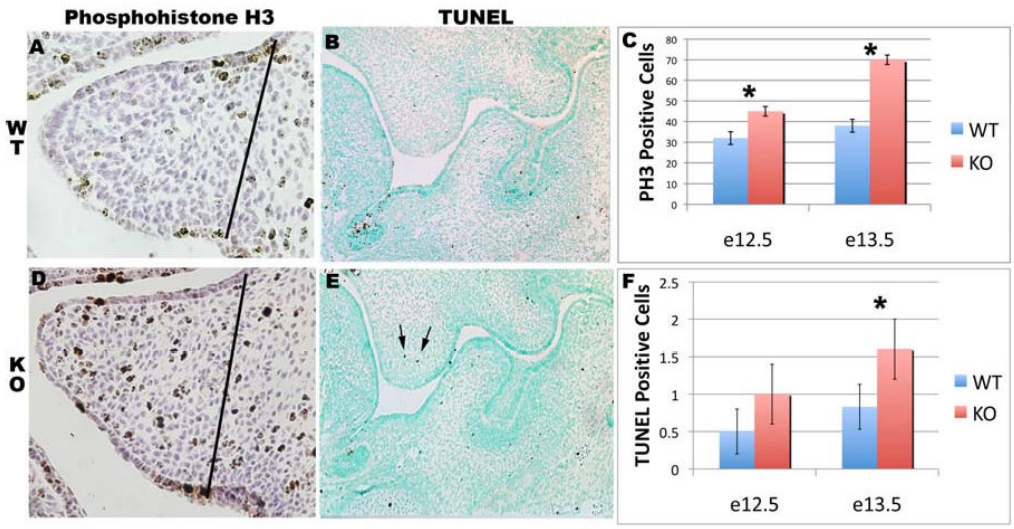

Figure 5. Alteration of proliferation and apoptosis in *Tbx1*-/- palates

Coronal sections through wild type (A) and *Tbx1*-/-(D) palate shelves at E13.5 stained with phosphohistone H3. (C) Graphical representation of palate proliferation at E12.5 and E13.5. Coronal sections through wild type (B) and *Tbx1* -/-(E) E13.5 palate shelves stained with TUNEL kit (arrow=TUNEL positive cell). (F) Graphical representation of palate apoptosis at E12.5 and E13.5. The dotted lines indicates the area of the palate counted. (*=Statistical significance)

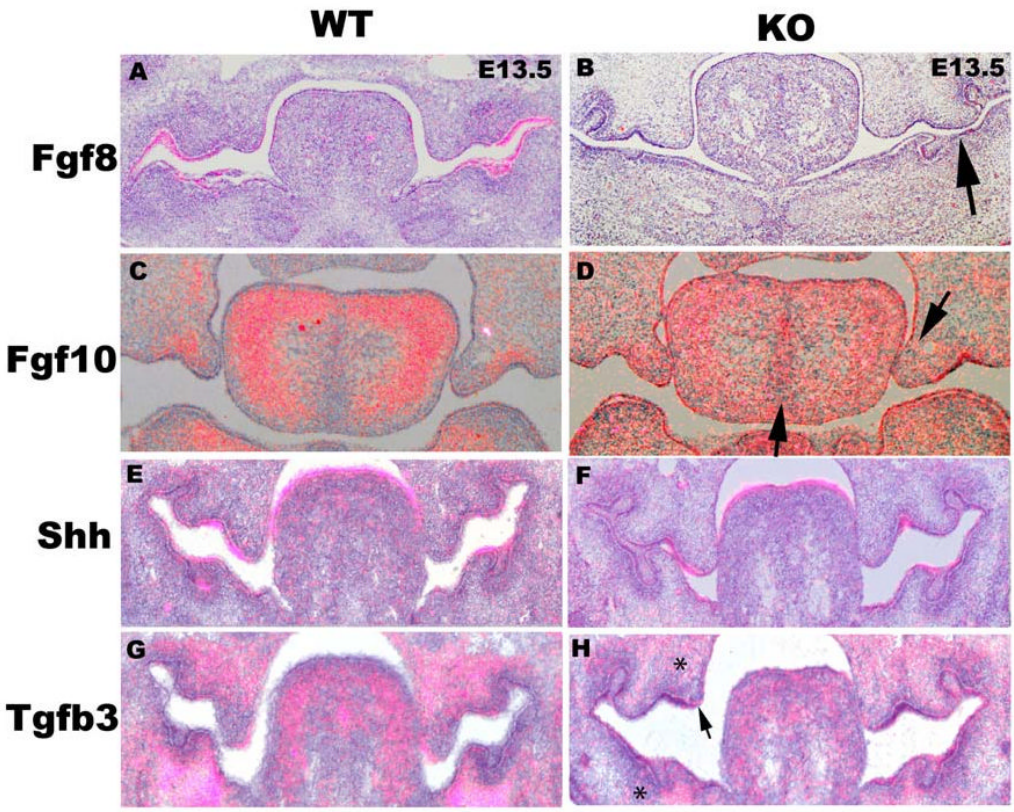

Figure 6. Diminished expression of *Fgf8* and increased expression of *Fgf10* in *Tbx1*-/- palate shelves

Coronal sections of situ hybridization with an *Fgf8* probe on E13.5 wild type (A) and *Tbx1*-/- (B) mice palates (note diminished *Fgf8* expression (arrow)). There is increased *Fgf10* expression in the midline of the tongue and the nasal side of the *Tbx1*-/- palate shelves (C, D). There is no change in gene expression comparing wild type mice with E13.5 *Tbx1*-/- mice for *Shh* (E, F), but there is decreased *Tgfb3* expression in the mandibular and skull base mesenchyme (*) but maintained MEE expression (arrow)(G, H).